

# Blue and violet graviton spectra from a dynamical refractive index

Massimo Giovannini <sup>1</sup>

*Department of Physics, CERN, 1211 Geneva 23, Switzerland*

*INFN, Section of Milan-Bicocca, 20126 Milan, Italy*

## Abstract

We show that the spectral energy distribution of relic gravitons mildly increases for frequencies smaller than the  $\mu\text{Hz}$  and then flattens out whenever the refractive index of the tensor modes is dynamical during a quasi-de Sitter stage of expansion. For a conventional thermal history the high-frequency plateau ranges between the mHz and the audio band but it is supplemented by a spike in the GHz region if a stiff post-inflationary phase precedes the standard radiation-dominated epoch. Even though the slope is blue at intermediate frequencies, it may become violet in the MHz window. For a variety of post-inflationary histories, including the conventional one, a dynamical index of refraction leads to a potentially detectable spectral energy density in the kHz and in the mHz regions while all the relevant phenomenological constraints are concurrently satisfied.

---

<sup>1</sup>Electronic address: massimo.giovannini@cern.ch

Relic gravitons are copiously produced in the early Universe because of the pumping action of the background geometry [1]. If a conventional stage of inflationary expansion is suddenly replaced by a radiation-dominated epoch, the spectral energy density in critical units at the present conformal time  $\tau_0$  (denoted hereunder by  $\Omega_{gw}(\nu, \tau_0)$ ) is quasi-flat [2] for comoving frequencies<sup>2</sup>  $\nu$  ranging, approximately, between 100 aHz and 100 MHz. The transition across the epoch of matter-radiation equality leads to an infrared branch where  $\Omega_{gw}(\nu, \tau_0) \propto \nu^{-2}$  between the aHz and 100 aHz [2]. If the post-inflationary plasma is stiffer than radiation (i.e. characterized by a barotropic index  $w = p/\rho$  larger than 1/3) the corresponding spectral energy density inherits a blue (or even violet) slope for typical frequencies larger than the mHz and smaller than about 100 GHz [3].

Gravitational waves might however acquire an effective index of refraction when they travel in curved space-times [4] and their spectral energy distribution becomes comparatively larger than in the conventional situation [5]. If the refractive index increases during a quasi-de Sitter stage of expansion, the propagating speed diminishes and  $\Omega_{gw}(\nu, \tau_0) \propto \nu^{n_T}$  (with  $n_T > 0$ ) for  $\nu$  ranging between 100 aHz and 100 MHz (recall that 1 aHz =  $10^{-18}$ Hz). There are no compelling reasons why there should be a single increasing branch extending throughout the whole range of variation of the comoving frequency. On the contrary we shall show that there are regions in the parameter space where all the phenomenological constraints are concurrently satisfied while the spectral energy distribution is only blue in the intermediate frequency range (roughly speaking below the  $\mu$ Hz) while it flattens out (and it may even decrease) around the mHz band. Depending on the post-inflationary thermal history the high-frequency plateau may reach out deep into the audio band and beyond.

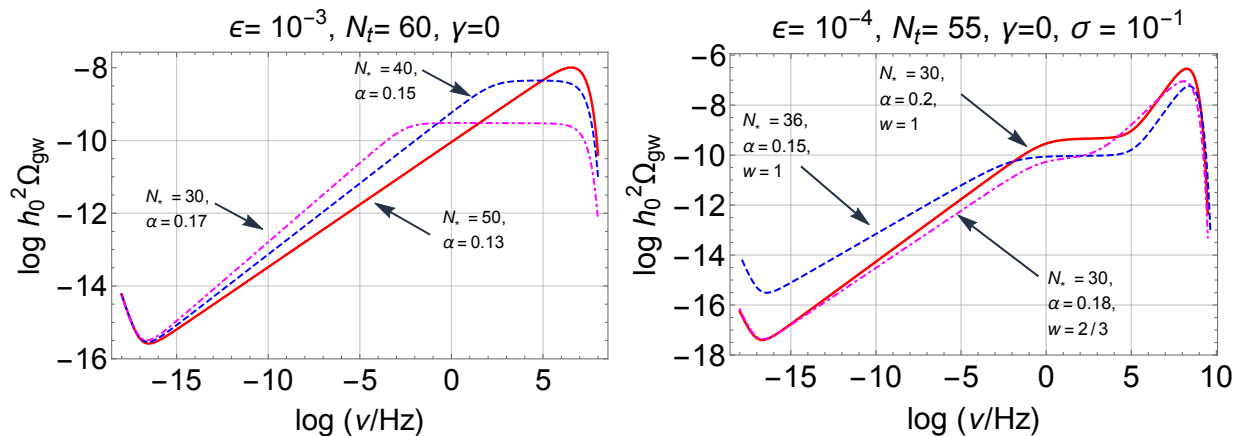


Figure 1: The spectral energy distribution of the relic gravitons produced by the variation of the refractive index during inflation is illustrated as a function of the comoving frequency for two broad classes of post-inflationary evolutions. The energy density is measured in critical units and common logarithms are employed on both axes.

<sup>2</sup>The scale factor shall be normalized throughout as  $a(\tau_0) = a_0 = 1$ . Hence, within the present notations, comoving and physical frequencies do coincide at the present time.

The spectral energy distribution of the relic gravitons produced by the variation of the refractive index is illustrated in Fig. 1 where, in both plots,  $N_t$  and  $N_* = a_*/a_i \leq N_t$  denote, respectively, the total and the critical number of e-folds beyond which the refractive index goes back to 1. Note also that  $\epsilon$  is the slow-roll parameter while  $\gamma$  is a parameter appearing in the modified action for the tensor modes in the presence of a dynamical refractive index (see below Eq. (3) and discussion therein). While the explicit evolution may vary [4, 5], the results of Fig. 1 refer to the situation where the refractive index evolves as a power of the scale factor  $a$  during inflation<sup>3</sup> i.e.  $n(a) = n_*(a/a_*)^\alpha$  for  $a < a_*$ , while  $n(a) \rightarrow 1$  when  $a > a_*$ . An explicit profile with this property is  $n(x) = (n_*x^\alpha e^{-\xi x} + 1)$  where  $x = a/a_*$ ;  $\xi$  controls the sharpness of the transition and we shall bound the attention to the case  $\xi > 1$  (in practice  $\xi = 2$  even if larger values of  $\xi$  do not change the conclusions reported here).

According to Fig. 1, if  $N_*$  is just slightly smaller than  $N_t$  the spectral energy density is increasing in the whole range of comoving frequencies between<sup>4</sup>  $\nu_{eq} = \mathcal{O}(100)$  aHz and  $\nu_{\max} = \mathcal{O}(200)$  MHz. As soon as  $N_*$  diminishes substantially,  $\Omega_{gw}(\nu, \tau_0)$  develops a quasi-flat plateau whose slope is controlled by the slow-roll parameter  $\epsilon$  (see dashed and dot-dashed curves in the left plot of Fig. 1). The knee and the end point of the spectral energy distribution are fixed by the typical frequencies  $\nu_*$  and  $\nu_{\max}$ :

$$\nu_* = p(\alpha, \epsilon, N_*, N_t) \nu_{\max}, \quad p(\alpha, \epsilon, N_*, N_t) = \left| 1 + \frac{\alpha}{1 - \epsilon} \right| e^{N_*(\alpha+1) - N_t}, \quad (1)$$

$$\nu_{\max} = 1.95 \times 10^8 \left( \frac{\epsilon}{0.001} \right)^{1/4} \left( \frac{\mathcal{A}_{\mathcal{R}}}{2.41 \times 10^{-9}} \right)^{1/4} \left( \frac{h_0^2 \Omega_{R0}}{4.15 \times 10^{-5}} \right)^{1/4} \text{ Hz}, \quad (2)$$

where  $\mathcal{A}_{\mathcal{R}}$  denotes the amplitude of the power spectrum of curvature inhomogeneities at the wavenumber  $k_p = 0.002 \text{ Mpc}^{-1}$  [6, 7] corresponding to the pivot frequency  $\nu_p = k_p/(2\pi) = 3.092$  aHz that defines the infrared band of the spectrum. In the right plot of Fig. 1 the spike at the end of the quasi-flat plateau is characterized by the frequency  $\nu_{spike} = \nu_{\max}/\sigma > \nu_{\max}$  (with  $\sigma < 1$ ) extending into the GHz band. This occurrence reminds of the conventional situation when the refractive index is not dynamical: in this case the value of the end-point frequency of the spectrum depends on the post-inflationary thermal history [3] and may exceed  $\nu_{\max} = \mathcal{O}(200)$  MHz. All in all Fig. 1 demonstrates that the spectral energy density may consist of two, three or even four different branches: the infrared branch (between the aHz and 100 aHz) is supplemented by a second mildly increasing branch extending between  $10^{-16}$  Hz and 200 MHz. Furthermore, when the variation of the refractive index terminates before the end of inflation a third branch develops between  $\nu_*$  and  $\nu_{\max}$ . Finally if the post-inflationary evolution is dominated, for some time, by a stiff barotropic fluid, then a fourth branch arises between few kHz and the GHz region.

<sup>3</sup>The rate of variation of the refractive index during the inflationary stage of expansion is given by  $\alpha$  in units of the Hubble rate; note also that, by definition,  $n_* = n_i(a_*/a_i)^\alpha$  with  $n_i = 1$ .

<sup>4</sup>Note that  $k_{eq} = 0.0732 [h_0^2 \Omega_{R0}/(4.15 \times 10^{-5})]^{-1/2} h_0^2 \Omega_{M0} \text{ Mpc}^{-1}$  where  $\Omega_{M0}$  and  $\Omega_{R0}$  are the values of the critical fractions of matter and radiation in the concordance paradigm;  $h_0$  denotes the present value of the Hubble rate  $H_0$  in units of 100 km/(sec  $\times$  Mpc). If  $h_0^2 \Omega_{M0} = 0.1411$  [6, 7],  $\nu_{eq} = k_{eq}/(2\pi) = \mathcal{O}(100)$  aHz.

The results summarized by Fig. 1 follow from the action describing the evolution of the tensor modes of the geometry in the presence of a dynamical refractive index [4, 5]:

$$S = \frac{1}{8\ell_P^2} \int d^3x \int d\tau a^2 n^{2\gamma} \left[ \partial_\tau h_{ij} \partial_\tau h_{ij} - \frac{\partial_k h_{ij} \partial^k h_{ij}}{n^2} \right], \quad \ell_P = \sqrt{8\pi G} = \frac{1}{M_P}, \quad (3)$$

where  $a(\tau)$  denotes the scale factor of a conformally flat geometry of Friedmann-Robertson-Walker type<sup>5</sup> and, as already mentioned,  $n(\tau)$  is the index of refraction. The parameter  $\gamma$  accounts for different possible parametrization of the effect: for instance, motivated by the original suggestion of Ref. [4], the first paper of Ref. [5] suggested an action (3) with  $\gamma = 0$ ; after this analysis some other authors (see e.g. second and third papers of Ref. [5]) considered a model with  $\gamma = 1$ . These two cases are just related by a conformal rescaling. Moreover for a generic case  $\gamma \neq 0$  the slope of  $\Omega_{gw}(\nu, \tau_0)$  is the one obtainable for  $\gamma = 0$  up to a  $\gamma$ -dependent prefactor that can be tacitly absorbed in a redefinition of the spectral index. Thus, even if the pivotal case is  $\gamma = 0$  Eq. (3) encompasses all the different possibilities and accounts for their physical equivalence.

For immediate convenience the conformal time coordinate  $\tau$  can be traded for the newly defined  $\eta$ -time whose explicit definition is  $n(\eta)d\eta = d\tau$ ; in the  $\eta$ -parametrization Eq. (3) becomes:

$$S = \frac{1}{8\ell_P^2} \int d^3x \int d\eta b^2(\eta) \left[ \partial_\eta h_{ij} \partial_\eta h_{ij} - \partial_k h_{ij} \partial^k h_{ij} \right], \quad b(\eta) = a n^{\gamma-1/2}. \quad (4)$$

Note that Eqs. (3)–(4) reproduce the results of Ref. [8] in the limit  $n \rightarrow 1$ . Furthermore, since  $n(a)$  goes back to 1 before the end of inflation,  $\eta$  and  $\tau$  eventually coincide in the post-inflationary phase so that the system can be directly quantized and solved in the  $\eta$ -time where the mode expansion for the field operator reads:

$$\hat{h}_{ij}(\vec{x}, \eta) = \frac{\sqrt{2}\ell_P}{(2\pi)^{3/2}b(\eta)} \sum_\lambda \int d^3k e_{ij}^{(\lambda)}(\vec{k}) \left[ f_{k,\lambda}(\eta) \hat{a}_{\vec{k}\lambda} e^{-i\vec{k}\cdot\vec{x}} + f_{k,\lambda}^*(\eta) \hat{a}_{\vec{k}\lambda}^\dagger e^{i\vec{k}\cdot\vec{x}} \right]. \quad (5)$$

In Eq. (5)  $\lambda = \oplus, \otimes$  runs over the tensor polarizations but, as in the conventional situation, the evolution of the mode functions is the same for each of the two values of  $\lambda$ :

$$\ddot{f}_k + \left[ k^2 - \frac{\ddot{b}}{b} \right] f_k = 0, \quad \dot{f} = \frac{\partial f}{\partial \eta} \equiv \frac{1}{n} \frac{\partial f}{\partial \tau} = \frac{f'}{n}. \quad (6)$$

The overdot denotes here a derivation with respect to  $\eta$  (*not* with respect to the cosmic time coordinate, as often tacitly assumed) while the prime denotes, as usual, a derivation with respect to the conformal time coordinate  $\tau$ . Simple algebra shows that  $\ddot{b}/b = \mathcal{F}^2 + \dot{\mathcal{F}}$ ; note that  $\mathcal{F} = \dot{b}/b$  coincides with  $\mathcal{H} = a'/a$  in the limit  $n \rightarrow 1$  by virtue of the basic relation  $n(\eta)d\eta = d\tau$  that connects Eqs. (3) and (4).

<sup>5</sup>More specifically  $\bar{g}_{\mu\nu} = a^2(\tau)\eta_{\mu\nu}$  and  $\eta_{\mu\nu} = \text{diag}(1, -1, -1, -1)$  is the Minkowski metric.

Equation (6) is equivalent to an integral equation with initial conditions assigned at  $\eta_{ex}$ , where  $\eta_{ex}$  is the turning point defined by the condition  $k^2 = \ddot{b}_{ex}/b_{ex}$ :

$$f_k(\eta) = \frac{b}{b_{ex}} \left\{ f_k(\eta_{ex}) + \left[ \dot{f}_k(\eta_{ex}) - \mathcal{F}_{ex} f_k(\eta_{ex}) \right] \int_{\eta_{ex}}^{\eta} \frac{b_{ex}^2}{b^2(\eta_1)} d\eta_1 - k^2 b_{ex} \int_{\eta_{ex}}^{\eta} \frac{d\eta_1}{b^2(\eta_1)} \int_{\eta_{ex}}^{\eta_1} b(\eta_2) f_k(\eta_2) d\eta_2 \right\}. \quad (7)$$

When  $\eta < \eta_*$  (i.e.  $N_t < N_*$ ) we have that  $b(\eta) = b_*(-\eta/\eta_*)^{-\delta}$  where  $b_* = a_* n_*^{\gamma-1/2}$  and  $\delta = [2 + \alpha(2\gamma - 1)]/[2(1 + \alpha - \epsilon)]$ ; in this regime  $\ddot{b} \neq 0$  so that the turning point is  $k\eta_{ex} = \mathcal{O}(1)$  and  $\eta_{ex} \simeq 1/k$ . Similarly, when  $a > a_*$  we have  $\ddot{b}/b = a''/a \simeq (2 - \epsilon)/[\tau^2(1 - \epsilon)^2]$  so that, again,  $k\tau_{ex} = \mathcal{O}(1)$ . If the reentry takes place when  $\ddot{b} \neq 0$  the relevant turning points are determined by the condition  $k^2 = |\ddot{b}_{re}/b_{re}|$ , i.e.  $k\eta_{re} = \mathcal{O}(1)$ . However, if the reentry occurs during a radiation-dominated stage of expansion, Eq. (6) implies instead  $\ddot{b} = a'' \rightarrow 0$ : since the curvature coupling vanishes in the vicinity of the second turning point  $\tau_{re}$  the condition  $k^2 = \ddot{b}_{re}/b_{re} \rightarrow 0$  implies  $k\eta_{re} \ll 1$  (and not, as it could be naively guessed,  $k\eta_{re} = \mathcal{O}(1)$ ).

From Eq. (7) the spectral energy distribution can be analytically estimated by matching the lowest-order solution across  $\eta_{re}$  and by evaluating the obtained result when the corresponding wavelengths are all shorter than the Hubble radius at the present epoch:

$$\Omega_{gw}(k, \tau_0) = \frac{k^4}{12H^2 \overline{M}_P^2 a^4 \pi^2} \left[ 1 + \left( \frac{\mathcal{F}_{ex}}{k} \right)^2 \right] \left( \frac{b_{re}}{b_{ex}} \right)^2 \left[ 1 + b_{ex}^4 \mathcal{J}^2(\eta_{ex}, \eta_{re}) \right], \quad (8)$$

$$\mathcal{J}(\eta_{ex}, \eta_{re}) = \int_{\eta_{ex}}^{\eta_{re}} \frac{d\eta_1}{b^2(\eta_1)}. \quad (9)$$

Whenever  $\eta_{ex} < \eta_*$  (and the reentry takes place during radiation), Eqs. (8)–(9) imply that  $\Omega_{gw} \propto \nu^{\bar{n}_T}$  where<sup>6</sup>  $\bar{n}_T = 2(1 - \delta) \equiv [\alpha(3 - 2\gamma) - 2\epsilon]/(1 + \alpha - \epsilon)$ : this is the slope appearing in both plots of Fig. 1 for  $\nu < \nu_*$ . Conversely, if  $\eta_{ex} > \eta_*$  (and the reentry takes place during radiation) the spectral energy density scales as  $\Omega_{gw} \propto \nu^{-2\epsilon}$ : this is the quasi-flat slope illustrated in both plots of Fig. 1 for  $\nu > \nu_*$ . Finally the MHz branch depends on the post-inflationary thermal history which modifies the spectrum whenever  $\eta_{re}$  does not fall within the radiation epoch: indeed the presence of a stiff phase preceding the radiation stage introduces a further branch corresponding to the modes reentering after the end of inflation and before the radiation dominance. In this branch spectral index is  $\bar{n}_T = [4 - 2/(1 - \epsilon) - 4/(3w + 1)]$ ; if, for instance,  $w \rightarrow 1$  the spectral index becomes explicitly  $\bar{n}_T \rightarrow 1 + \mathcal{O}(\epsilon)$ : this is, incidentally, the slope of  $\Omega_{gw}(\nu, \tau_0)$  before the spike in the GHz band (see, in this respect, the right plot of Fig. 1).

Even though Eqs. (8) and (9) are central to the analytic estimates, an accurate assessment the cosmic graviton spectrum can be obtained in terms of the transfer function of the energy

---

<sup>6</sup>Note that since  $\epsilon < \alpha < 1$  the spectral index is given, to leading order, by  $\bar{n}_T \simeq (3 - 2\gamma)\alpha$ : as anticipated after Eq. (3) different values of  $\gamma$  simply rescale the value of  $\alpha$ .

density<sup>7</sup>. Across equality the transfer function is

$$T_{eq}(\nu, \nu_{eq}) = \sqrt{1 + c_{eq} \left(\frac{\nu_{eq}}{\nu}\right) + b_{eq} \left(\frac{\nu_{eq}}{\nu}\right)^2}. \quad (10)$$

To transfer the spectral energy density inside the Hubble radius Eqs. (6) and (7) are integrated numerically across equality and this procedure fixes the numerical coefficients  $c_{eq} = 0.5238$  and  $b_{eq} = 0.3537$  [8] and the typical frequency of the transition:

$$\nu_{eq} = 1.362 \times 10^{-17} \left(\frac{h_0^2 \Omega_{M0}}{0.1411}\right) \left(\frac{h_0^2 \Omega_{R0}}{4.15 \times 10^{-5}}\right)^{-1/2} \text{ Hz}. \quad (11)$$

The same procedure leading to Eqs. (10) and (11) gives the transfer function across the intermediate frequency  $\nu_*$  already introduced in Eq. (1):

$$T_*(\nu, \nu_*) = \left[1 + c_* \left(\frac{\nu}{\nu_*}\right)^{2\epsilon + n_T} + b_* \left(\frac{\nu}{\nu_*}\right)^{4\epsilon + 2n_T}\right]^{-1/2}, \quad (12)$$

while  $c_{eq}$  and  $b_{eq}$  can be accurately assessed,  $c_*$  and  $b_*$  depend on the parametrization of the refractive index but are of order 1. Finally the transfer function across  $\nu_s$  determines the high-frequency branch of the spectrum

$$T_s(\nu, \nu_s) = \sqrt{1 + c_s \left(\frac{\nu}{\nu_s}\right)^{p(w)/2} + b_s \left(\frac{\nu}{\nu_s}\right)^{p(w)}}, \quad p(w) = 2 - \frac{4}{3w + 1}, \quad (13)$$

$$\nu_s = \sigma^{3(w+1)/(3w-1)} \nu_{\max}, \quad \nu_{spike} = \nu_{\max}/\sigma, \quad \sigma = \left(\frac{H_{\max}}{H_r}\right)^{\frac{1-3w}{6(w+1)}}, \quad (14)$$

where  $H_r$  denotes the Hubble rate at the onset of the radiation-dominated phase and  $w$  is the barotropic index of the stiff phase. As in the case of  $c_*$  and  $b_*$  also  $c_s$  and  $b_s$  change depending on the values of  $w$ . In the case  $w \rightarrow 1$  there are even logarithmic corrections which have been specifically scrutinized in the past (see e.g. [3]); moreover the derivation of  $T_{eq}(\nu)$  and  $T_s(\nu)$ , in a different physical situation, has been discussed in detail in the last paper of Ref. [8].

Defining therefore  $\mathcal{T}(\nu, \nu_{eq}, \nu_*, \nu_s)$  as the total transfer function, the spectral energy distribution in critical units becomes:

$$h_0^2 \Omega_{gw}(\nu, \tau_0) = \mathcal{N}_\rho r_T(\nu_p) \mathcal{T}^2(\nu, \nu_{eq}, \nu_*, \nu_s) \left(\frac{\nu}{\nu_p}\right)^{n_T} e^{-2\beta\nu/\nu_{\max}}, \quad (15)$$

$$\mathcal{T}(\nu, \nu_{eq}, \nu_*, \nu_s) = T_{eq}(\nu, \nu_{eq}) T_*(\nu, \nu_*) T_s(\nu, \nu_s), \quad (16)$$

$$\mathcal{N}_\rho = 4.165 \times 10^{-15} \left(\frac{h_0^2 \Omega_{R0}}{4.15 \times 10^{-5}}\right) \left(\frac{\mathcal{A}_{\mathcal{R}}}{2.41 \times 10^{-9}}\right), \quad (17)$$

---

<sup>7</sup>It is customary to introduce the transfer function of the power spectrum and the transfer function of the energy density. Although the two concepts are complementary, the latter turns out to be more useful than the former when dealing with the cosmic graviton spectrum (see, in particular, the last paper of Ref. [8] for a complete discussion of the problem).

where  $n_T = [\alpha(3 - 2\gamma) - 2\epsilon]/(1 + \alpha - \epsilon)$  and  $r_T(\nu_p)$  is the tensor to scalar ratio evaluated at the pivot frequency  $\nu_p$ :

$$r_T(\nu) = \epsilon \frac{2^{6-n_T}}{\pi} \Gamma^2\left(\frac{3-n_T}{2}\right) e^{q_T} \left|1 + \frac{\alpha}{1-\epsilon}\right|^{2-n_T} \left(\frac{\nu}{\nu_{\max}}\right)^{n_T}, \quad (18)$$

$$q_T = (3 - 2\gamma - n_T)(N_*\alpha - \ln n_i) + n_T(N_t - N_*). \quad (19)$$

In the conventional case  $r_T(\nu_p)$  is related to the slow-roll parameter  $\epsilon$  and to the tensor spectral index  $n_T$  via the so-called consistency relations which are however not enforced in the present situation. When the refractive index is not dynamical (i.e.  $\alpha \rightarrow 0$  and  $\gamma \rightarrow 0$ ) it is nonetheless true that  $n_T \rightarrow -2\epsilon$ , as expected. Finally the parameter  $\beta = \mathcal{O}(1)$  appearing in Eq. (15) depends upon the width of the transition between the inflationary phase and the subsequent radiation dominated phase; by using different widths we can estimate  $0.5 \leq \beta \leq 6.3$  [8]: the results on slopes of the four branches are not affected by the value of  $\beta$  which however controls the rate of exponential suppression after the endpoint frequency.

According to Eq. (10),  $T_{eq}(\nu) \rightarrow 1$  for  $\nu \gg \nu_{eq}$  however the effect of neutrino free-streaming introduces a minor source of supplementary suppression in the range  $\nu_{eq} < \nu < \nu_{bbn}$  where  $\nu_{bbn}$  denotes the nucleosynthesis frequency (i.e.  $\nu_{bbn} = \mathcal{O}(10^{-11})$  Hz). The neutrino free-streaming produces an effective anisotropic stress leading ultimately to an integro-differential equation<sup>8</sup> [9]. This effect is not central to the present discussion but it can be easily included; similarly another potential effect is associated with the variation of the effective number of relativistic species; in the case of the minimal standard model this would imply that the reduction will be  $\mathcal{O}(0.38)$  (see e.g. the last paper of Ref. [3]). Note finally that if the various scales only reenter during radiation we have that  $T_s(\nu) \rightarrow 1$  (or, more formally,  $\nu_s \rightarrow \infty$  for a fixed comoving frequency  $\nu$ ).

The parameters of the cosmic graviton spectra illustrated in Fig. 1 have not been randomly guessed but they are consistent with the phenomenological constraints and with some basic detectability requirements that will now be elucidated. In the low-frequency range the tensor to scalar ratio of Eq. (18) is bounded from above not to conflict with the observed temperature and polarization anisotropies of the Cosmic Microwave Background; we specifically required  $r_T(\nu_p) < 0.06$ , as it follows from a joint analysis of Planck and BICEP2/Keck array data [7]. The pulsar timing measurements impose instead a limit at the frequency  $\nu_{pulsar} \simeq 10^{-8}$  Hz (roughly corresponding to the inverse of the observation time along which the pulsars timing has been monitored [10]) and implying  $\Omega_{gw}(\nu_{pulsar}, \tau_0) < 1.9 \times 10^{-8}$ . Finally the big-bang nucleosynthesis sets an indirect constraint on the extra-relativistic species (and, among others, on the relic gravitons) at the time when light nuclei have been formed [11]. This constraint is often expressed in terms of  $\Delta N_\nu$  representing the contribution of

---

<sup>8</sup>If the only collisionless species are the neutrinos (which are massless in the concordance paradigm), the amount of suppression of  $h_0^2 \Omega_{gw}$  can be parametrized by the function  $\mathcal{F}(R_\nu) = 1 - 0.539R_\nu + 0.134R_\nu^2$ . This means that we are talking about a figure of the order of  $\mathcal{F}^2(0.405) = 0.645$  (for  $N_\nu = 3$  and  $R_\nu = 0.405$ ).

supplementary (massless) neutrino species (see e.g. [12]) but the extra-relativistic species do not need to be fermionic. If, as in our case, the additional species are relic gravitons we will have to demand that:

$$h_0^2 \int_{\nu_{bbn}}^{\nu_{\max}} \Omega_{gw}(\nu, \tau_0) d \ln \nu = 5.61 \times 10^{-6} \Delta N_\nu \left( \frac{h_0^2 \Omega_{\gamma 0}}{2.47 \times 10^{-5}} \right). \quad (20)$$

The bounds on  $\Delta N_\nu$  range from  $\Delta N_\nu \leq 0.2$  to  $\Delta N_\nu \leq 1$  so that the right hand side of Eq. (20) turns out to be between  $10^{-6}$  and  $10^{-5}$ . The shaded areas of Fig. 2 illustrate the

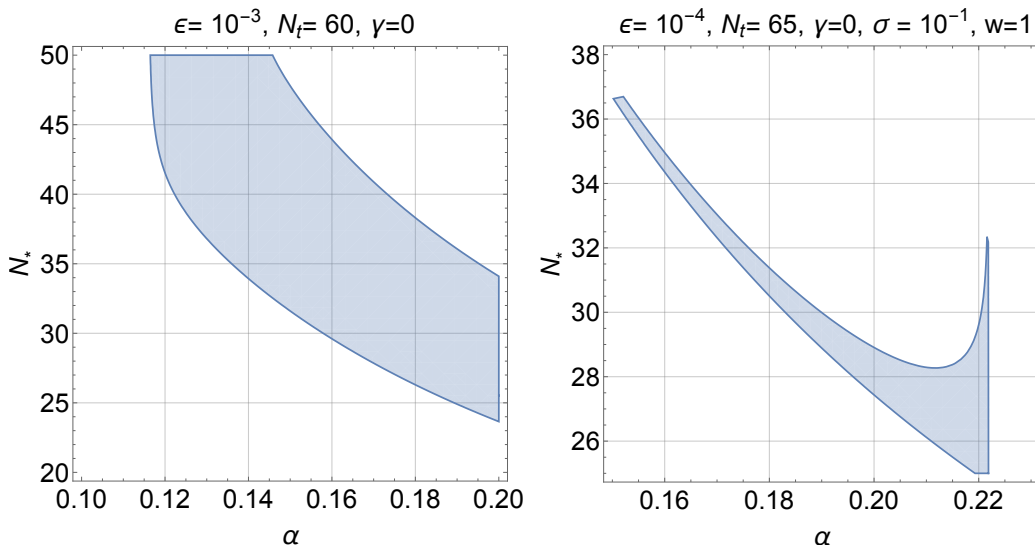


Figure 2: In the shaded regions the phenomenological constraints are all satisfied and the corresponding spectral energy density leads to a potentially detectable signal both in the mHz and in the kHz bands.

regions where not only the phenomenological constraints are concurrently satisfied but the spectral energy density is also potentially detectable both in the mHz band (i.e.  $0.1 \text{ mHz} < \nu_{\text{mHz}} < \text{Hz}$ ) and in the audio band (i.e.  $\text{Hz} < \nu_{\text{audio}} < 10 \text{ kHz}$ ). In particular we required  $h_0^2 \Omega_{gw}(\nu_{\text{audio}}, \tau_0) \geq 10^{-10}$  hoping that (in a not too distant future) the Ligo/Virgo detectors in their advanced configurations will reach comparable sensitivities [13]. With a similar logic we are led to require  $h_0^2 \Omega_{gw}(\text{mHz}, \tau_0) \geq 10^{-12}$  in the mHz band always assuming that comparable sensitivities will be reached by space-borne interferometers [14] which are, at the moment, only proposed and not yet operational. In the left plot of Fig. 2 we illustrate the case where all the modes reenter during radiation while in the right plot we consider the presence of a stiff phase preceding the ordinary radiation epoch. In case the onset of the radiation-dominated phase is delayed by the presence of a stiff phase; a spike appears in the GHz region and the signal is comparatively more constrained: this is the reason why the area of the left plot is larger than the area of the right plot. This kind of signal might however be interesting for electromagnetic detectors of gravitational radiation which have



been proposed and partially developed through the past decade [15]. As anticipated the parameters of the two plots of Figs. 1 have been drawn, respectively, from the shaded areas of the two plots illustrated in Fig. 2.

The inflationary scenarios based on a quasi-de Sitter stage of expansion suggest that the spectral energy distribution of the cosmic gravitons should always decrease in frequency and hence remain below  $10^{-17} \rho_{crit}$  both in the mHz and in the kHz bands. If the refractive index of the tensor modes is dynamical  $\Omega_{gw}(\nu, \tau_0)$  develops an increasing branch at intermediate frequencies while it flattens out above the  $\mu\text{Hz}$  region with an approximate amplitude that can exceed the conventional signal even by nine orders of magnitude. In this case the quasi-flat plateau present in the conventional situation gets larger and it is pushed at higher frequencies. All in all the increase of the spectral energy density does not conflict with the limits applicable to the cosmic graviton backgrounds and leads to potential signals both in the audio and in the mHz windows. If the onset of the radiation epoch is delayed by a post-inflationary phase with equation of state stiffer than radiation, the spectral energy density inherits a further spike in the GHz region. Potentially detectable signals can then be expected both for terrestrial interferometers and for space-borne detectors provided the refractive index is dynamical at least for a limited amount of time during an otherwise conventional quasi-de Sitter stage of expansion.

It is a pleasure to acknowledge useful discussions with F. Fidecaro. The author wishes also to thank T. Basaglia, A. Gentil-Beccot and S. Rohr of the CERN Scientific Information Service for their kind assistance.

## References

- [1] L. P. Grishchuk, Sov. Phys. JETP **40**, 409 (1975) [Zh. Eksp. Teor. Fiz. **67**, 825 (1974)]; Annals N. Y. Acad. Sci. **302**, 439 (1977); A. A. Starobinsky, JETP Lett. **30**, 682 (1979) [Pisma Zh. Eksp. Teor. Fiz. **30**, 719 (1979)].
- [2] V. A. Rubakov, M. V. Sazhin and A. V. Veryaskin, Phys. Lett. **115B**, 189 (1982); B. Allen, Phys. rev. D **37**, 2078 (1988); V. Sahni, Phys. Rev. D **42**, 453 (1990); L. P. Grishchuk and M. Solokhin, Phys. Rev. D **43**, 2566 (1991); M. Gasperini and M. Giovannini, Phys. Lett. B **282**, 36 (1992); Phys. Rev. D **47**, 1519 (1993).
- [3] M. Giovannini, Phys. Rev. D **58**, 083504 (1998); Phys. Rev. D **60**, 123511 (1999); Class. Quant. Grav. **16**, 2905 (1999); Class. Quant. Grav. **26**, 045004 (2009).
- [4] P. Szekeres, Annals Phys. **64**, 599 (1971); P. C. Peters, Phys. Rev. D **9**, 2207 (1974).
- [5] M. Giovannini, Class. Quant. Grav. **33**, 125002 (2016) [arXiv:1507.03456 [astro-ph.CO]]; Y. Cai, Y. T. Wang and Y. S. Piao, Phys. Rev. D **93**, 063005 (2016) [arXiv:1510.08716 [astro-ph.CO]]; Phys. Rev. D **94**, 043002 (2016) [arXiv:1602.05431 [astro-ph.CO]]; M. Giovannini, CERN-TH-2018-107 [arXiv:1803.05203 [gr-qc]].

- [6] G. Hinshaw *et al.* [WMAP Collaboration], *Astrophys. J. Suppl.* **208**, 19 (2013); C. L. Bennett, *et al.* [WMAP Collaboration], *Astrophys. J. Suppl.* **208**, 20B (2013).
- [7] P. A. R. Ade *et al.* [Planck Collaboration], *Astron. Astrophys.* **571**, A22 (2014); *Astron. Astrophys.* **571**, A16 (2014); P. A. R. Ade *et al.* [BICEP2 and Keck Array Collaborations], *Phys. Rev. Lett.* **116**, 031302 (2016) [arXiv:1510.09217 [astro-ph.CO]].
- [8] L. H. Ford and L. Parker, *Phys. Rev. D* **16**, 1601 (1977); *Phys. Rev. D* **16**, 245 (1977); B. L. Hu and L. Parker, *Phys. Lett A* **63**, 217 (1977); M. Giovannini, *Class. Quant. Grav.* **26** 045004 (2009).
- [9] S. Weinberg, *Phys. Rev. D* **69**, 023503 (2004); D. A. Dicus and W. W. Repko, *Phys. Rev. D* **72**, 088302 (2005); L. A. Boyle and P. J. Steinhardt, *Phys. Rev. D* **77**, 063504 (2008); Y. Watanabe and E. Komatsu, *Phys. Rev. D* **73**, 123515 (2006).
- [10] V. M. Kaspi, J. H. Taylor, and M. F. Ryba, *Astrophys. J.* **428**, 713 (1994); W. Zhao, *Phys. Rev. D* **83**, 104021 (2011) [arXiv:1103.3927 [astro-ph.CO]]; P. B. Demorest *et al.*, *Astrophys. J.* **762**, 94 (2013) [arXiv:1201.6641 [astro-ph.CO]].
- [11] V. F. Schwartzmann, *JETP Lett.* **9**, 184 (1969); M. Giovannini, H. Kurki-Suonio and E. Sihvola, *Phys. Rev. D* **66**, 043504 (2002) [astro-ph/0203430]; R. H. Cyburt, B. D. Fields, K. A. Olive, and E. Skillman, *Astropart. Phys.* **23**, 313 (2005) [astro-ph/0408033].
- [12] M. Dentler, A. Hernandez-Cabezudo, J. Kopp, P. Machado, M. Maltoni, I. Martinez-Soler and T. Schwetz, arXiv:1803.10661 [hep-ph].
- [13] J. Aasi *et al.* [LIGO Scientific Collaboration], *Class. Quant. Grav.* **32**, 074001 (2015) [arXiv:1411.4547 [gr-qc]]; F. Acernese *et al.* [VIRGO Collaboration], *Class. Quant. Grav.* **32**, 024001 (2015) [arXiv:1408.3978 [gr-qc]]; Y. Aso *et al.* [KAGRA Collaboration], *Phys. Rev. D* **88**, no. 4, 043007 (2013).
- [14] P. Amaro-Seoane *et al.*, *GW Notes* **6**, 4 (2013); G. M. Harry, P. Fritschel, D. A. Shaddock, W. Folkner, E. S. Phinney, *Class. Quant. Grav.* **23** 4887 (2006); S. Kawamura *et al.*, *Class. Quant. Grav.* **28**, 094011 (2011).
- [15] A. M. Cruise, *Class. Quantum Grav.* **17** , 2525 (2000); F. Y. Li, M. X. Tang and D. P. Shi, *Phys. Rev. D* **67**, 104008 (2003); R. Ballantini, P. Bernard, A. Chincarini, G. Gemme, R. Parodi and E. Picasso, *Class. Quant. Grav.* **21**, S1241 (2004); A. M. Cruise and R. M. Ingley, *Class. Quantum Grav.* **23**, 6185 (2006); A. Nishizawa *et al.*, *Phys. Rev. D* **77**, 022002 (2008).